Heliyon 10 (2024) e38599

Contents lists available at ScienceDirect

Heliyon

journal homepage: www.cell.com/heliyon

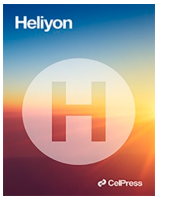

Research article

Promoting diabetic oral mucosa wound healing with a light-responsive hydrogel adaptive to the microenvironment

Shuwen Ding [a,1], Xiaohui Zhang [b,c,1], Gaopeng Wang [b,c], Jiaying Shi [a], Jiayu Zhu [a], Jiayu Yan [a], Jing Wang [b,c,**], Junhua Wu [a,*]

[a] *Department of Prosthodontics, Stomatological Hospital and Dental School of Tongji University, Shanghai Engineering Research Center of Tooth Restoration and Regeneration, Shanghai, PR China*
[b] *State Key Laboratory of Bioreactor Engineering, East China University of Science and Technology, Shanghai, 200237, PR China*
[c] *Engineering Research Center for Biomedical Materials of Ministry of Education, East China University of Science and Technology, Shanghai, 200237, PR China*

ARTICLE INFO

Keywords:
Diabetic oral wounds
Angiogenesis
Macrophages
Sulfated chitosan

ABSTRACT

In diabetic patients, compromised angiogenesis due to endothelial dysfunction leads to delayed intraoral wound healing. However, the moist and dynamic environment of the oral cavity impedes the use of normal wound dressings. Sulfated chitosan (SCS) is a promising biomaterial that promoting angiogenesis. Here, a light-responsive hydrogel combined with SCS explored intraoral wound healing. We designed a SCS-modified hydrogel combined with alginate Methacryloyl (AlgMA) and acrylamide (AM) and demonstrated efficient wet adhesion and mechanical properties suitable for the wet and dynamic oral environment. *In vitro*, the SAA hydrogel improved the tube formation of human umbilical vein endothelial cells (HUVECs) under high-glucose conditions. Further investigations revealed that the SAA hydrogel can regulate HUVEC-macrophage interactions, leading to a shift in macrophage polarization from M1 to M2, thereby fostering an environment conducive to angiogenesis under high-glucose condition. The results demonstrated the substantial therapeutic impact of the SAA hydrogel on diabetic oral defect repair by effectively enhancing the local blood supply and angiogenesis.

1. Introduction

In diabetic patients, compromised angiogenesis resulting from endothelial dysfunction leads to delayed intraoral wound healing. The global rise in diabetes mellitus cases and its associated complications has placed a significant burden on both public health and socioeconomic systems [1]. Delayed wound healing, a common complication of diabetes mellitus, is typically characterized by a prolonged inflammatory phase and impaired angiogenesis [2]. Under normal physiological condition, neutrophils secrete cytokines, growth factors and various potent antimicrobial agents following tissue injury. During the pre-inflammatory phase, macrophages primarily exhibit the M1 phenotype and express proinflammatory markers. In the post inflammatory phase, macrophages mainly

* Corresponding author.
** Corresponding author. State Key Laboratory of Bioreactor Engineering, East China University of Science and Technology, Shanghai, 200237, PR China.
E-mail addresses: wangjing08@ecust.edu.cn (J. Wang), wujunhua_sh@tongji.edu.cn (J. Wu).
[1] These authors contributed equally to this work.

https://doi.org/10.1016/j.heliyon.2024.e38599
Received 12 June 2024; Received in revised form 24 September 2024; Accepted 26 September 2024
Available online 28 September 2024

display the M2 phenotype and secrete anti-inflammatory cytokines essential for wound healing, such as IGF-1 and TGF-β. However, in diabetes, excessive inflammation hinders the transition of macrophages to the M2 phenotype, as evidenced by increased levels of IL-1β, TNF-α, and MMP-9 [3]. Persistent glycolipid metabolic abnormalities in diabetic patients trigger the release of inflammatory mediators, leading to prolonged infiltration of cells such as monocyte macrophages and neutrophils. Additionally, the apoptosis of these cells is delayed, further increasing the levels of inflammatory mediators. As a result, the body remains in a state of chronic inflammation, hindering the formation of granulation tissue [4].

During the proliferative phase of wound healing under normal conditions, the blood vessel density reaches its peak, surpassing that of healthy skin. As healing progresses from the vascular phase to the stabilization phase, the expression of proangiogenic factors decreases, whereas the expression of antiangiogenic factors increases. This shift promotes endothelial cell apoptosis as well as the initiation of vascular maturation [5]. In contrast, diabetic individuals exhibit an impaired hypoxic response and reduced HIF-1 levels, resulting in decreased VEGF-α mRNA expression and increased PEDF production [6]. Moreover, the expression of Ang1/Ang 2/Tie2, another crucial angiogenic pathway independent of the VEGF/VEGFR2 axis, is diminished [7]. High glucose levels are believed to interfere with the surface mechanosensors of endothelial cells (ECs), altering their response to shear forces. This interference affects various biological functions, including proliferation, survival, migration, bioactive substance synthesis, thrombosis prevention, tubulogenesis, and endothelial marker expression [8]. Animal studies suggest that diabetic rats experience early and prolonged delay in oral soft tissue wound healing compared to non-diabetic rats. This delay is characterized by slower wound closure, reduced angiogenesis and alterations in multinucleated macrophage numbers [9]. Furthermore, research indicated that diabetes decreases salivary EGF levels in both humans and mice, potentially hindering oral wound healing [10]. Diabetic children have also been found to have lower levels of salivary antimicrobial peptides, such as histones [11]. Reduced histone level may adversely affect keratinocyte migration and diminish the effectiveness of antimicrobial defenses in diabetic patients [12].

The healing process of oral soft tissue wounds in diabetic patients resembles that of skin wounds, characterized by a delayed inflammatory response and impaired angiogenesis [13]. Soft tissues of the maxillofacial region can be damaged by trauma, infections, and maxillofacial tumors [14]. The impaired angiogenesis and prolonged inflammatory phase associated with diabetes mellitus exacerbate the difficulty of healing these wounds [13]. Moreover, most maxillofacial soft tissue injuries have irregular shapes and occur within the unique, moist, and dynamic environment of the oral cavity [15]. Consequently, there is a critical need for a versatile material that can conform to various defect shapes, possesses wet adhesion properties, and provide targeted therapeutic actions against the diabetic microenvironment for treating maxillofacial soft tissue injuries in clinical settings.

Most current research on treatments for chronic diabetic wounds has focused on skin tissues, with few studies conducted on oral soft tissue defects related to diabetes mellitus. For instance, a zinc alginate hydrogel loaded with RL-QN15 peptides in hollow silica nanoparticles, which showed enhanced biocompatibility, antimicrobial properties, and accelerated wound healing by promoting cell proliferation and vascular regeneration in chronic wound treatments [17]. Common topical treatments, such as powders, solutions, ointments and tablets are often rapidly diluted or washed away with saliva [16]. Existing bio-gels present challenges in oral mucosal treatment: fibrin gels bind poorly to moist tissues [19], cyanoacrylate gels are inflexible and harmful [18], and NHS ester- and DOPA-based bio-gels require complex handling and are environmentally sensitive [20]. Thus, one of the biggest challenges in treating oral mucosal defects is the development of hydrogel dressings that adhere tightly to wet tissue and are both bioavailable and biocompatible.

Sulfated chitosan (SCS), similar to heparin and distinguished by its sulfonic acid group, can modulate vascularization and inflammation during bone repair by altering the transition of M1 macrophages to M2 macrophages, thus exhibiting anti-inflammatory and vasculogenic properties [21,22]. However, it remains uncertain whether SCS can improve the function of impaired endothelial cells in the healing of diabetic wounds.

In this study, a SAA hydrogel was constructed using a one-step rapid method. The letters “S", “A" and “A" represent SCS, alginate methacryloyl (AlgMA), and acrylamide (AM), respectively. As a result of Lithium Phenyl (2,4,6-trimethylbenzoyl)phosphonate (LAP) action, the double bonds in AM and AlgMA begin to polymerize, forming a cross-linked, three-dimensional network. By copolymerizing AM and AlgMA, the hydrogel exhibited good mechanical properties, wet adhesive capability, and biocompatibility. Upon light-curing for 5 s, the SAA hydrogel isolates the defect from external elements. The efficacy of the SAA hydrogel in enhancing wound healing *in vivo* was tested in a diabetic rat model with oral mucosal defects. Additionally, the interaction of the hydrogel with macrophages and endothelial cells under high-glucose conditions was examined *in vitro* cell model.

2. Materials and methods

2.1. Synthesis and characterization of hydrogels

2.1.1. Synthesis and preparation of hydrogels

Sulfonated chitosan (SCS) (Mw = 17,174; degree of sulfation = 65 %) was synthesized according to the previous method [23]. Subsequently, AlgMA and AM were combined and the photo initiator LAP was added to the mixture. Briefly, SCS was dissolved in a neutral phosphate-buffered saline (PBS) solution at a concentration of 1 mg/ml to prepare the SCS stock solution. AM was dissolved in a neutral 0.05 % LAP solution at concentrations of 10 %, 15 %, and 30 %, vortexed for 10 s, and then set aside. AlgMA sourced from Aladdin Reagent Co. (Shanghai) was prepared in a similar manner in the AM solution, mixed at 4 °C overnight, and sonicated for 3 min to eliminate air bubbles, resulting in the AlgMA-AM solution. Hydrogel precursor solutions with different SCS concentrations of 0.64 μg/ml, 1.64 μg/ml, and 2.64 μg/ml. The AlgMA-AM hydrogel precursor was exposed to UV light for 5 s. When the solution solidified, it was extracted from the mold for tensile testing, freeze-drying, and SEM scanning to determine the final AM concentration.

2.1.2. SEM analysis

The microstructure of the hydrogel samples was characterized via SEM (PHENOM-PRO, USA). Before imaging, the lyophilized hydrogel samples were coated with a thin layer of gold/palladium. Images were subsequently captured at an accelerating voltage of 15 kV and recorded at various magnifications.

2.1.3. Adhesion test

2.1.3.1. Pigskin lap shear experiments. To assess the bio adhesive qualities of hydrogels, lap-shear tests were conducted to measure the adhesive strength across hydrogels with different AM concentrations and Yiketie®. Hydrogels were applied on fresh pig skin and subjected to UV illumination until cured, covering a bond area of 10 mm × 10 mm. Samples were stretched to the point of failure using a universal testing machine (Instron 5567) at a crosshead speed of 1 mm/min until detachment occurred. Bond strength was determined by dividing the peak load by the initial bonding area. Three specimens per group were tested to ascertain the bond strength (n = 3).

2.1.3.2. SEM analysis. To evaluate the binding of the tissue to the hydrogel, the hydrogel was applied to fresh rat mucosal tissue. Samples were then freeze-dried, dehydrated, and examined using a gold-palladium coated scanning electron microscope.

2.1.3.3. Histological staining. To assess the adhesion between the tissue and the hydrogel, the hydrogel was administered to fresh rat mucosal tissue. The samples were freeze-drying and embedded in optimal cutting temperature (OCT), sectioned and stained with hematoxylin and eosin (HE), and the interaction sites between the material and mucosa were examined microscopically.

2.1.3.4. Tissue retention time of SAA hydrogels. To determine the duration ability of hydrogel retention within tissues, an *in vitro* model of the hard palate mucosa of a rat was developed. Rat hard palate samples were immersed in artificial saliva, which was stirred intermittently (12 h of stirring followed by 12 h of rest). The samples were then removed at 12, 24, and 48 h to assess material retention.

2.1.4. SAA hydrogel swelling rate test

To evaluate the swelling behavior, the synthesized SAA hydrogels were immersed in PBS at 37 °C with pH of 7.4 for 80 h. At specific time intervals, the hydrogels were retrieved and their weight was recorded (W_1). The initial weight of the sample (W_0) was measured, enabling the calculation of the swelling ratio using the formula:

Swelling ratio (%) = $W_1/W_0 \times 100$ %

2.1.5. Measurement of SCS loadings

To determine the optimal SCS loading, informed by prior experimental results, concentrations of 0.64 μg/ml, 1.64 μg/ml, and 2.64 μg/ml were selected. These were then evaluated for suitable SCS loading through *in vitro* cell scratch assays and *in vivo* studies of angiogenesis.

2.1.5.1. Preparation of hydrogel extracts. Glucose (Macklin, G6172) was dissolved in low-glucose DMEM medium (Cytiva). The solution was then filtered through a 0.22 μm filter (Biosharp) to produce a high-glucose medium with a final concentration of 30 mM, replicating diabetic conditions *in vitro* as per literature. Light-cured composite hydrogel samples with an SCS concentration of 1.64 μg/ml were incubated in both high-glucose and normal media within a cell culture incubator for 24 h following 2 h of UV irradiation to prepare SAA extracts with varying sugar levels. For coincubation, 0.1 g of hydrogel was combined with 1 ml of medium.

2.1.5.2. Scratch assay. The pro-migratory effect of the gel was examined with HUVECs. The cells were seeded into 6-well plates at a density of 1×10^5 cells per well. Upon reaching 90 % confluence, a 200 μL pipette tip was used to gently scrape the cells. The cells were subsequently washed three times with PBS to clear away any dislodged cellular debris from the DMEM. The hydrogel oligosaccharide extract (100 μg/mL, n = 3) was then added to the culture medium and coincubated with the cells for various durations. Cell migration was observed and images were taken under a Leica microscope (DMi1, Germany). Quantitative analysis of the scratched areas was performed using ImageJ software. The cell migration rate was determined using the formula:

Cell migration rate (%) = $[(A_0 - A_T)/A_0] \times 100\%$

(Where A_0 denotes the initial scratch area at 0 h and A_T denotes the scratch area at different times.)

2.2. Diabetic rat oral mucosa wound healing model

All animal procedures were approved by the Institute of Animal Care and Use Committee of Tongji University and complied with all relevant ethical regulations (no. [2023]-DW-48). All procedures involving male SD rats (180–220 g, 6–8 weeks old) adhered to the guidelines for the care and use of experimental animals. The diabetes model was induced via intraperitoneal injection of STZ (55 mg/kg). Blood glucose levels were monitored on the 1st, 7th, and 14th days via a glucometer; rats exhibiting levels above 16.7 mmol/L were classified as diabetic and included in further studies. Diabetic rats (n = 3) were randomly assigned to one of four groups: blank

control, AA, SAA, or iRegene®. Following anesthesia, a full-thickness wound measuring 1.5 mm in diameter was afflicted on the dorsum of each rat. Various hydrogels were then administered to the wounds. Adequate water and food were supplied, and the wound dressings were routinely changed. The wound area was quantitatively analyzed via ImageJ software.

Wound closure rate (%) = $[(A_0 - A_1)/A_0] \times 100\%$

(A_0 represents the day 1 wound area, and at represents the wound area at different times).

2.3. Histological and immunofluorescence staining

Oral mucosal samples were fixed in paraformaldehyde for one day at room temperature, embedded in paraffin, and subjected to hematoxylin and eosin (H&E) staining. For immunofluorescence staining, mucosal samples were blocked with goat serum for 30 min at room temperature and incubated overnight at 4 °C with primary antibodies: anti-CD31 (FAB3628G, R&D Systems, USA), anti-α-SMA (DF13357, Affinity, USA), and VEGF (ab150375, abcam, USA). Subsequently, the sections were incubated with matching secondary antibodies (Servicebio Co., Ltd., China) for 1 h, and cell nuclei were stained with DAPI (Beyotime, China) for 10 min in the dark. Ultimately, the immunofluorescence images were captured using confocal laser scanning microscopy (CLSM).

2.4. Biocompatibility evaluation

2.4.1. Cell counting Kit-8 (CCK-8) assay

The biocompatibility of the composite hydrogels was evaluated on human umbilical vein endothelial cells (HUVECs) and human periodontal ligament stem cells (hPDLSCs), via the Cell Counting Kit-8 (CCK-8) assay (Beyotime, C0038), in accordance with the manufacturer's instructions. Briefly, cells were seeded into 96-well plates and cocultured with various hydrogel extracts for 1, 3, and 5 days. To perform the CCK-8 assay, the culture medium and CCK-8 reagent were mixed in each well at a 9:1 ratio and incubated at 37 °C for 1 h. Optical density measurements were then obtained at a wavelength of 450 nm.

2.4.2. Live/dead cell staining

The cytotoxicity of the gel was evaluated using oral epithelial cells cocultured with various hydrogel extracts for 48 h via a Calcein AM/PI Double Stain Kit (MKBio, Shanghai, MX3012) in accordance with the manufacturer's instructions. Following the preparation of the assay and stain buffers, the cells were incubated with the stain buffer at 37 °C for 15 min. Fluorescent images were then captured using a confocal microscope (Nikon A1-Si).

2.5. Cell culture

Human umbilical vein endothelial cell (HUVECs) and RAW 264.7 cell lines were obtained from the American Type Culture Collection (ATCC). HUVECs and RAW 264.7 cells were cultured in Dulbecco's modified Eagle's medium (DMEM, Cytiva) supplemented with 10 % fetal bovine serum (FBS), while RAW 264.7 cells were cultured in DMEM-high glucose (Cytiva) containing 10 % FBS. All cells were maintained in a humidified cell culture incubator with 5 % CO2 at 37 °C.

2.6. Indirect coculture

Glucose anhydrose (Macklin, G6172) was dissolved in the culture medium (900 g/L). The solution was subsequently passed through a 0.22 μm filter (Biosharp) to generate high-glucose medium at a final concentration of 450 g/L to simulate diabetic conditions *in vitro*. The hydrogel samples were incubated in the culture medium at 37 °C for 24 h after 30min irradiation under ultraviolet light for sterilization. Then, the supernatants were extracted and filtered with a 0.22 μm filter and then mixed with the high-glucose medium (450 g/L) described previously at a ratio of 1:1. HUVECs and RAWs were cultured in DMEM/high glucose (Cytiva). After 24 h, the culture media of HUVECs and RAWs were removed and replaced with the above mixture (high-glucose medium and composite hydrogel supernatants) as high glucose group (HG group). Cells cocultured with SAA extract were taken as the low glucose group (LG group).

2.7. Migration experiments

The transwell assay was utilized to assess the migratory properties of HUVECs. In the transwell assay, HUVECs were suspended in serum-free medium at a density of 5 × 10^3 cells/mL, and 100 μL of this suspension was placed into the upper chamber of 24-well plates (Corning, USA) with an 8.0 μm polycarbonate membrane. The lower chamber was filled with medium supplemented under various conditions, similar to those in cell proliferation assays. After 24 h of incubation at 37 °C with 5 % CO2, cells on the upper side of the microporous membrane were removed, and the cells that had migrated were stained with 0.1 % crystal violet for 7 min. An optical microscope was subsequently employed to observe the stained cells and to capture images.

2.8. Tube formation assay

To investigate capillary network formation, a tube formation assay was conducted. Initially, Matrigel (354,230, Corning, USA) was thawed at 4 °C overnight. It was then evenly distributed across the bottom of 96-well plates (50 μL per well) and incubated (5 % CO_2, 37 °C) for 30 min to solidify into a gel. Subsequently, HUVECs were plated onto the gel surface (1×10^5 cells/well) and incubated at 37 °C with 5 % CO2. Different hydrogel extracts served as the medium for HUVECs. After 6 h, the medium was discarded and the wells were gently rinsed with PBS. The HUVECs were then examined using a fluorescent microscope (Ti-U, Nikon, Japan) and analyzed with Image J software.

2.9. Total RNA extraction

A total of 1 mL of TRIzol reagent (Takara) was utilized to lyse cell or oral mucosa tissue, followed by a 5-min incubation at room temperature to dissociate nucleoprotein complexes. The lysates were then transferred to an Eppendorf microcentrifuge tube, and 0.2 mL of chloroform was added to facilitate homogenization. After a 3-min incubation at room temperature, the samples were centrifuged at 12,000 rpm for 15 min at 4 °C. The upper aqueous phase was carefully transferred to a new tube, and an equal volume of isopropanol was added to precipitate the RNA. Following a 10-min incubation at room temperature, the samples were centrifuged again at 12,000 rpm for 10 min at 4 °C. The supernatants were carefully removed, and the RNA pellets were washed with 75 % ethanol. The samples were then centrifuged at 7500 rpm for 5 min at 4 °C, and the ethanol was subsequently removed. The RNA pellets were air-dried for 10 min at room temperature and reconstituted in 20 μL of RNase-free water.

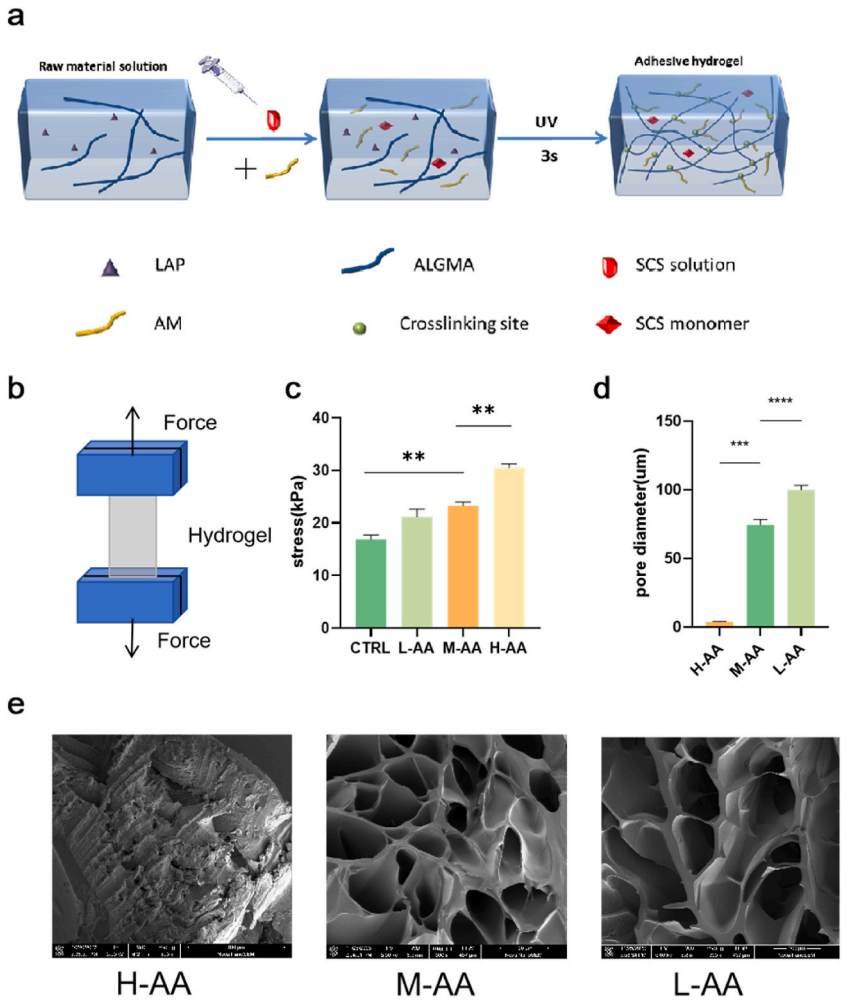

Fig. 1. Mechanical properties and Structural characterization of AA hydrogels. (a) The design strategy and application of the SAA hydrogel. (b) images showing the AA hydrogel during stretching. (c) Average tensile strength of AA hydrogels with different AA ratios. (d) SEM and (e) diameter analysis of AA freeze-dried hydrogels with different AA ratios (*$p < 0.05$, **$P < 0.01$, ***$P < 0.005$, ****$P < 0.001$).

2.10. qRT-PCR analysis

Total RNA was extracted from cells (6-well plates, 5 × 105 cells/well) and rat oral mucosa using TRIzol Reagent (Takara Biomedical Technology Co., Ltd., Japan), following the manufacturer's instructions. The relative RNA expression levels of the target gene were evaluated using qRT-PCR.

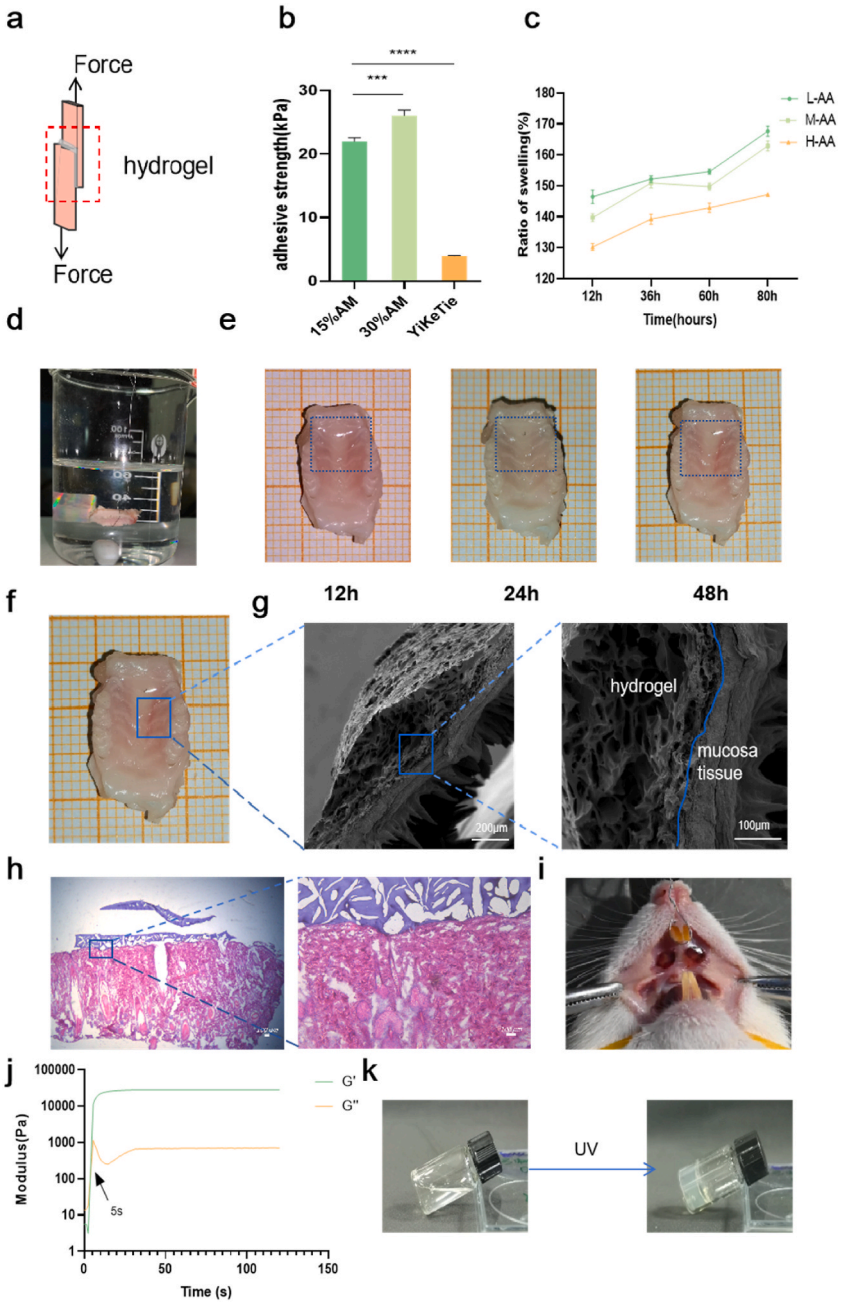

Fig. 2. Adhesion properties and other characterizations of AA hydrogels. (a) Porcine skin adhesive strength test via standard lap shear measurements. (b) Adhesive strength of hydrogels with different ratios of AM. (c) Swelling ratio of the AA hydrogels. (d) Schematic diagram of the *in vitro* device for simulating the oral environment. (e–f) Photographs of AA hydrogel dressings in a simulated food flow. (g) SEM and (h) HE staining observation of the integration of the AA hydrogel with rat oral mucosal tissues. (i) Images of the AA hydrogel applied in oral wound areas of diabetic rats. (j) Storage modulus (G′) and loss modulus (G″) analyses of AA hydrogels during gelation process (37 °C, frequency: 1.0 Hz, Strain:1.0 %). (k) Sol-gel phase transition photographs of the AA hydrogel at room temperature (*$P < 0.05$, **$P < 0.01$, ***$P < 0.005$, ****$P < 0.001$).

2.11. Data analysis

All quantitative data were analyzed with GraphPad Prism 8 and are presented as mean values ± SEM. Significant differences between two groups were assessed using an unpaired *t*-test, while multiple comparisons were analyzed with one-way ANOVA followed by Dunnett's test. Symbols *, **, *** and **** represent $P < 0.05$, $P < 0.01$, $P < 0.005$, and $P < 0.001$, respectively.

3. Results and discussion

3.1. Synthesis and characterization of SAA hydrogels

AlgMA was employed as a cross-linking agent to synthesize AlgMA-AM hydrogels through the chemical reaction between the double bonds of AM and AlgMA. SCS solution was incorporated and formed hydrogen bonds with AlgMA-AM, as depicted in Fig. 1. The SAA hydrogel precursor solution was prepared via a one-step method and various concentrations of AM, AlgMA, and SCS were incorporated. Following light curing, the tensile properties of AM-AlgMA hydrogels were evaluated across a range of AM concentrations. An increase in AM concentration resulted in a corresponding increase in the average tensile strength of the AA hydrogels. The AM-AlgMA hydrogels displayed average tensile strengths (Fig. 1b and c) of 18.52 kPa, 22.34 kPa, and 24.09 kPa at AM concentrations of 0 %, 10 %, and 15 %, respectively. When the AM concentration was increased to 30 %, the tensile strength (Fig. 1b and c) of the AA

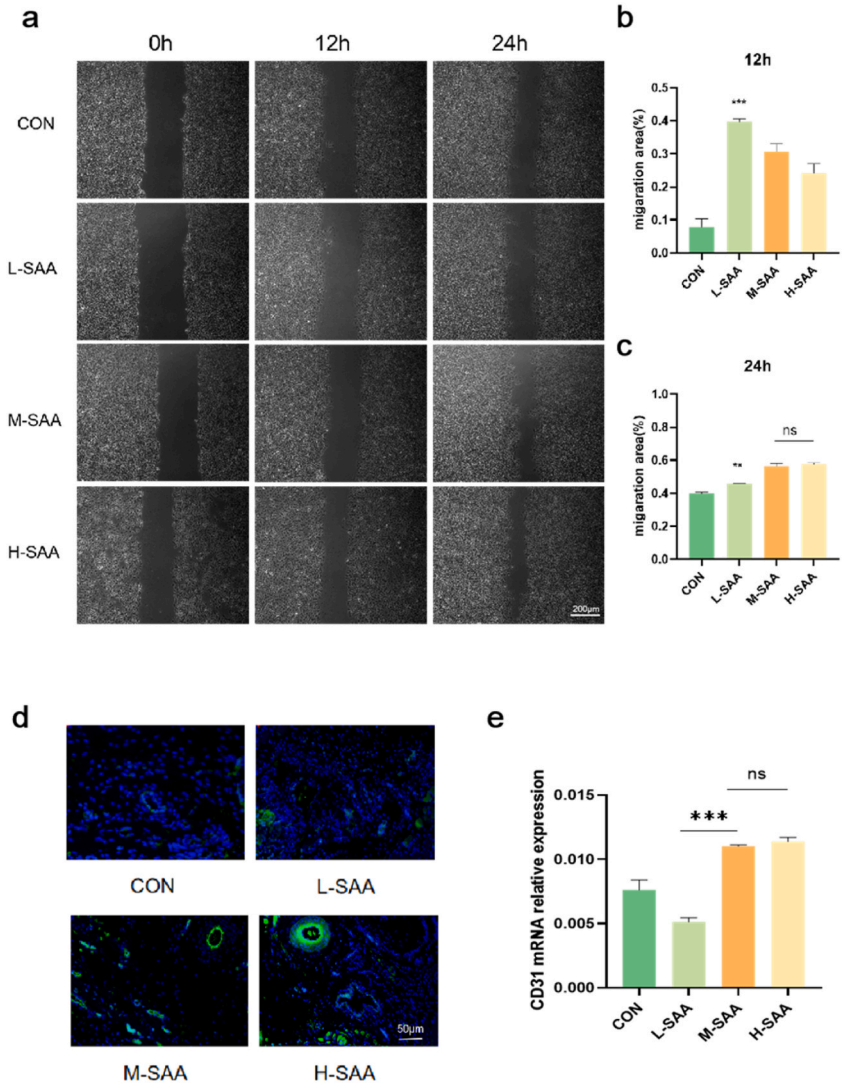

Fig. 3. Angiogenesis performance of SAA hydrogels loaded with different SCS concentrations. (a–c) Cell scratch assay was performed to assess the migration ability of HUVECs from different groups and quantitative analysis. (d) CD31-stained blood vessels in diabetic rat oral mucosa defects regions. (e) CD31 expression in the diabetic rat oral mucosa defect regions (*$P < 0.05$, **$P < 0.01$, ***$P < 0.005$, ****$P < 0.001$).

hydrogels reached its peak at 31.98 kPa, highlighting the positive influence of higher AM concentrations on tensile strength. The gels exhibited superior tensile strength, surpassing commercial fibrin glue in all tested conditions [24]. The improved performance can be attributed to the flexibility of alginate, which enables adaptation to soft mucosal surfaces [25] as well as the role of AM in improving material toughness, tensile strength, and resistance to degradation by food or saliva. Scanning electron microscopy analysis (Fig. 1d and e) revealed that increasing the AM monomer concentration led to a significant reduction in the pore size of hydrogel, resulting in a denser structure. Hydrogels with low and medium AM concentrations presented cellular pore sizes that were favorable for cell adhesion and migration [26]. In contrast, larger pores exceeding 100 μm facilitated cell migration and transformation [27]. Pores ranging from 2 to 50 nm provide a large specific surface area, promoting increased drug loading and enhancing protein bioactivity through optimal conformation and contact surfaces [28].

Lap shear experiments were performed using moistened pigskin to investigate the adhesive strength of AA hydrogels with varying concentrations of AM in comparison to a commercial product, Yiketie®. The AA hydrogels with medium and high concentrations of AM exhibited no significant difference in adhesive performance (Fig. 2a and b), both surpassing the adhesive strength of the commercially available fibrin glue (15 kPa as referenced in Ref. [24]) and Yiketie® (approximately 4 kPa). On the basis of the findings from tensile testing, SEM pore analysis and lap shear experiments, the medium concentration of AM was chosen for subsequent experiments.

In an *in vivo* oral model, AA hydrogels with a medium concentration of AM were applied to rats' hard palates (Fig. 2d). After 48 h, the majority of the AA hydrogels remained intact (Fig. 2e). The swelling capabilities of AA hydrogels were assessed by immersing them in PBS solution (10.0 mM, pH = 7.4) for 12 h, 36 h, 60 h, and 80 h, respectively. The swelling ratio (Fig. 2c) demonstrated that all samples exhibited increased water absorption during the immersion period. Owing to the chemical crosslinking between AM and AlgMA, the weight of H-AA hydrogel increased by 1.6 times after 80 h. The H-AA hydrogel displayed an optimal swelling rate, enabling

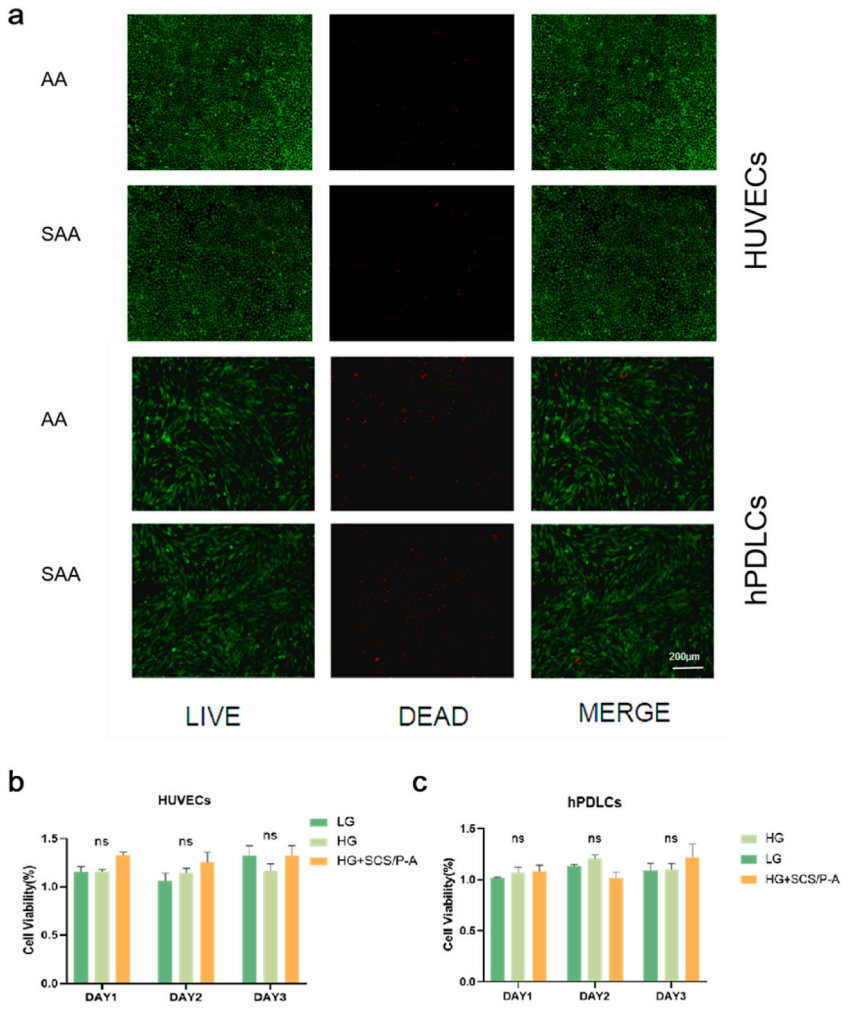

Fig. 4. Biocompatibility evaluation of the SAA hydrogel *in vitro*. (a) Live/dead cell assay of HUVECs and hPDLCs seeded on SAA hydrogels extraction. Scale bar = 200μm. The CCK-8 assay of (b) HUVECs and (c) hPDLCs cultured with hydrogel extraction (*$p < 0.05$, **$P < 0.01$, ***$P < 0.005$, ****$P < 0.001$).

effective bonding with the surrounding healthy tissue near the defect site. This property ensures that the hydrogel maintains its shape and stability, which is essential for successful tissue integration and overall healing [26]. Diabetic mucosal wounds are typically characterized by a prolonged inflammatory microenvironment with a weakly acidic pH [29]. In such an environment, the carboxyl (-COOH) groups within the AA hydrogel become more prevalent, facilitating hydrogen bonding and electrostatic interactions with the amino (-NH2) groups on the tissue surface. As a result, the AA hydrogel demonstrates adequate adhesive properties in diabetic mucosal wounds, indicating significant potential for wound healing applications. Furthermore, when the AA hydrogel was applied to oral mucosal defects in diabetic rats, rapid and robust adhesion was observed following UV light exposure. Electron microscopy (Fig. 2g) and hematoxylin and eosin (HE) (Fig. 2h) staining of the hydrogel-mucosa interface confirmed the formation of a secure bond between the mucosa and the SAA hydrogel. This adhesion can be attributed to the grafting of methacrylate (MA) groups onto the alginate backbone and the subsequent gelation in the presence of LAP as a photo initiator. Rheological tests indicated that the AA hydrogel transitions to a gel state within 5 s of light exposure but remains malleable when not cured, meeting clinical demands for efficient application.

To identify suitable SCS loadings for achieving the best angiogenic effect, the migration of HUVECs was evaluated using hydrogels with varying SCS concentrations. The impact of SAA hydrogel with different SCS concentrations on HUVEC migration (Fig. 3a) at the scratch wound's periphery was assessed. Based on previous experimental results [23], SAA hydrogels with different SCS concentrations were prepared in 48-well plates by adding 1 ml of complete medium (1 % PS, 5 % FBS and DMEM-basic), After a 24-h incubation, the extracts were collected and filtered. The data revealed that after 12 and 24 h of co-incubation with SAA hydrogel extracts, the SCS group exhibited increased mobility relative to the control group. At 12 h (Fig. 3b), HUVECs migrated more in the presence of low-concentration SAA (0.64 μg/ml) compared to high-concentration SAA (1.64 μg/ml and 2.64 μg/ml). However, at 24 h (Fig. 3c), higher SCS concentrations facilitated better HUVEC migration. To optimize SCS loading, *in vivo* tests were conducted by applying SAA hydrogels with varied SCS concentrations to diabetic rats' oral mucosal defects. Immunofluorescence (Fig. 3d and e) on day seven indicated that hydrogels with higher SCS concentrations (1.64 μg/ml) had enhanced vasculogenic effects. Considering the previous experiments, a final SCS loading of 1.64 μg/ml was selected.

3.2. SAA hydrogel exhibited favorable cell compatibility

The cytotoxicity of the SAA hydrogels was assessed by culturing human umbilical vein endothelial cells (HUVECs) and human periodontal ligament cells (hPDLCs) with SAA hydrogel extracts. The results of cell counting kit-8 (CCK-8) assay and live/dead cell staining revealed consistent cell viability following coculture with composite hydrogel extracts (Fig. 4a, b, c). As anticipated, the SAA hydrogel had no effect on cell apoptosis, confirming its safety for cell survival. The gel components are derived from natural sources and do not contain any potentially toxic substances. Additionally, the noncovalent gelation process does not produce any side effects. Therefore, the composite gel is considered safe for biological applications (see Fig. 5).

3.3. SAA hydrogel promotes angiogenesis of high-glucose treated HUVECs

To simulate the hyperglycemic environment in diabetic patients, human umbilical vein endothelial cells (HUVECs) were cultured in DMEM medium with a glucose concentration of 30 mM for 24 h, following literature guidelines [30]. The qPCR results revealed reduced expression of angiogenesis-related factors (including FGF1, FGF2, ANG1 and VEGF) in endothelial cells cultured with high glucose for 24 h. Additionally, the CCK-8 assay results showed no significant difference in HUVEC proliferation (Fig. 4b and c) between HG-treated HUVECs and HG-SAA-treated HUVECs groups compared to blank control group. Thus, HG and HG-SAA treatments do not affect the normal proliferation rate of HUVECs.

Angiogenesis involves cell proliferation, migration and tube formation. The tube formation and migration abilities of HUVECs damaged by high sugar were assessed by SAA hydrogel through tube formation and Transwell assays.

Inadequate angiogenesis plays an important role in the pathogenesis of diabetic wound healing and microvascular disease [31]. Angiogenic factors include anti-angiogenic and pro-angiogenic factors. Under normal conditions, these factors maintain a stable functional vascular network. However, in the diabetic microenvironment, the expression of angiogenesis-related factors is reduced and result in lower angiogenesis levels than normal [32].

Transwell assay results demonstrated that fewer HUVECs migrated in the high glucose group than in the control group. Compared to the high-glucose group, adding AA hydrogel extracts did not significantly alter migration. However, coincubation with SAA hydrogel extracts increased the number of migrating cells in high-glucose-treated HUVECs.

In summary, the SAA hydrogel improves the tube-forming and migrating abilities of HG-treated HUVECs.

3.4. Effect of SAA hydrogel on angiogenesis and immunity in vitro

Dysfunctional angiogenesis often coincides with macrophage dysfunction in diabetic conditions [33]. During normal wound healing, macrophages transition from a proinflammatory to a prorepair phenotype, facilitating angiogenesis [34]. However, in diabetic wounds, macrophages struggle to adopt a reparative phenotype [35]. Coculturing an HG-SAA extract with macrophages revealed an early M1 polarization (at 12 h) followed by a late-phase M2 conversion (at 24 h) (Fig. 6b). These results are consistent with previous research demonstrating that SAA mitigates excessive inflammatory responses in mouse peritoneal macrophages, enhancing anti-inflammatory factor expression and promoting M2 polarization [21] (see Fig. 7).

Previous research on macrophage-endothelial cell interactions has demonstrated that macrophages play a crucial role in

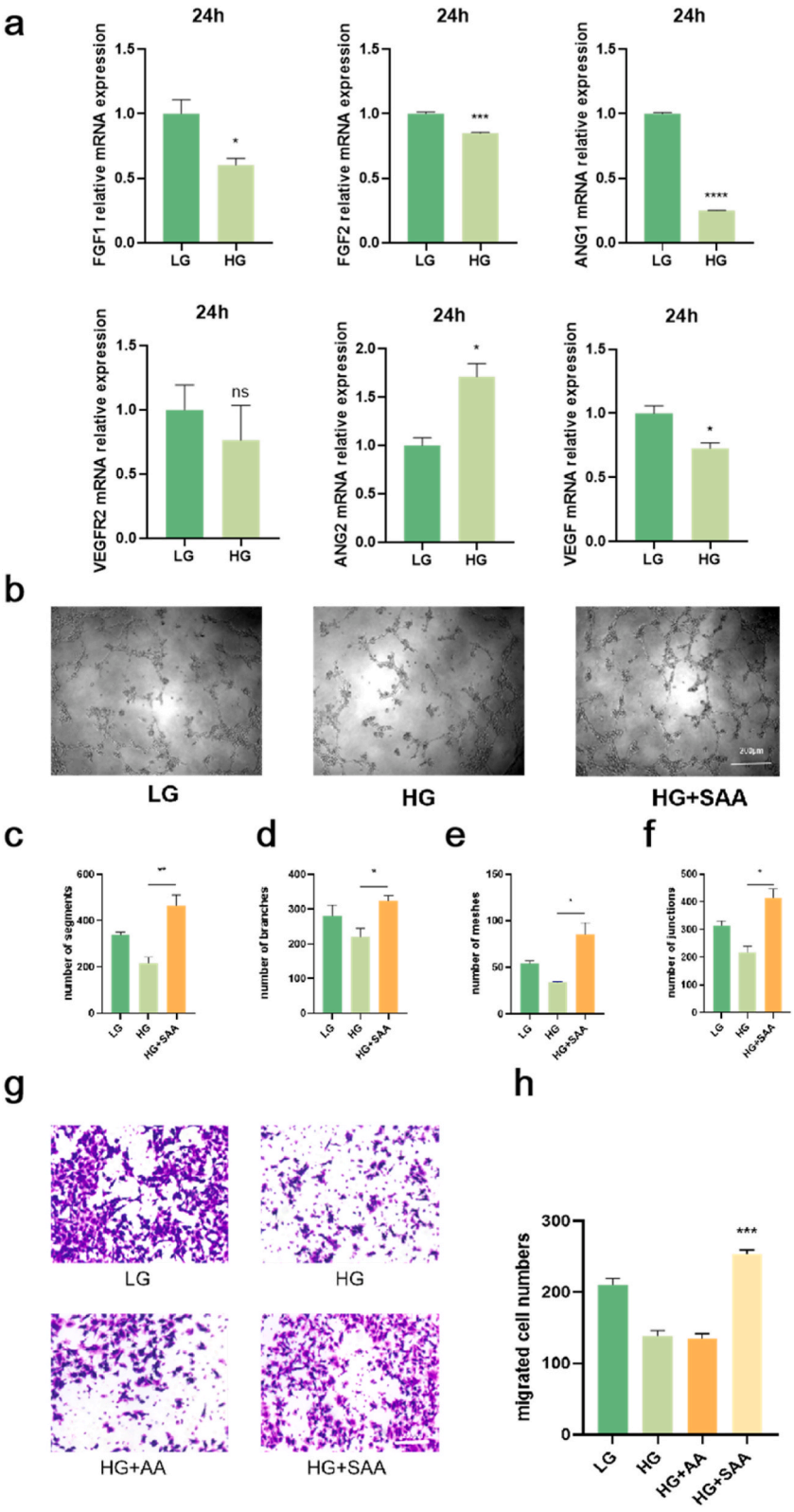

(caption on next page)

Fig. 5. SAA hydrogels improve the function of HG-treated HUVECs *in vitro*.(a) Decreased expression of angiogenic factors in high glucose-treated HUVECs. (b–f) Images of tube formation of HUVECs with different treatments and quantitative analysis of tube formation ability, Scale Bar: 200 μm. (g–h) The images of transwell of HUVECs with different treatments and quantitative analysis of transwell ability, Scale Bar: 200 μm (*$p < 0.05$, **$P < 0.01$, ***$P < 0.005$, ****$P < 0.001$).

maintaining endothelial integrity. Macrophages regulate endothelial cell (EC) metabolism, function, vascular growth, germination, angiogenesis, and regeneration. Additionally, macrophages influence endothelial cell proliferation, migration, and other phenotypic behaviors [36]. To investigate potential interactions between SAA hydrogel and macrophages in regulating endothelial cell phenotypes, a coculture system was established (Fig. 6j). The results (Fig. 6k–p) demonstrated that HUVECs cultured in RAW-conditioned medium exhibited up-regulated expression of VEGF, FGF1, FGF2, ANG1, and ANG2. Vascular endothelial growth factor (VEGF) is one of the most common vascular endothelial growth factors and is the most specific growth factor for the vascular endothelium. VEGF has been shown to be an essential regulator of normal angiogenesis and neovascularization. Ang1 is a potent vascular maturation factor that stabilizes pericytes and endoplasmic cells in capillaries. In contrast, Ang-2 is an autocrine cytokine produced by endothelial cells that acts as an antagonist of Ang1/Tie2 signaling and is involved in the remodeling of the vascular system, thus promoting VEGF-dependent angiogenesis [39]. Angiogenesis can also be mediated by the angiopoietin (Ang1-2)/Tie-2 pathway independently of the VEGF pathway [40]. The results showed that effect of the SAA hydrogel on immune response regulation could further promote the expression of angiogenic genes in HUVECs.

In another co-culture system *in vitro*, HUVECs were exposed to SAA hydrogel in a high-glucose environment, resulting in altered expression levels of relevant angiogenic genes. Using qRT-PCR, the expression of angiogenic genes in HUVECs was analyzed (Fig. 6a). Notably, the SAA hydrogel group exhibited lower gene expression levels of ANG1, ANG2, FGF2, and FGF1 compared with the AA-treated group. In a high-glucose environment, the results suggest that SAA hydrogel promotes the expression of VEGF in HUVECs, the most predominant angiogenic gene, whereas the expression levels of other relevant angiogenic factors were not improved.

Angiogenesis contributes to immune microenvironment regulation [37]. Endothelial cells play a crucial role in determining macrophage fate. They can serve as macrophage niches, influencing macrophage phenotype, activation, polarization, and differentiation during immune responses and inflammation [38].

We examined how the interaction between HUVECs and hydrogels affect the secretion of inflammatory factors by macrophages within the inflammatory microenvironment. Macrophages cultured in high glucose-conditioned medium from HUVECs presented increased expression of anti-inflammatory factors (such as CXCL2, CXCL5, and TGF-β) and decreased expression of pro-inflammatory factors (IL-1β and TNF-α). Notably, the chemokines CXCL2 and CXCL5 attract neutrophils and promote angiogenesis [39]. ELR-positive CXC chemokines CXCL2 and CXCL5 directly enhance endothelial cell migration and proliferation, which ultimately promotes neovascularization through interaction with CXCR2 [40]. These findings suggest that the SAA hydrogel acting on the HUVEC microenvironment may serve as an anti-inflammatory agent and contribute to tissue regeneration, potentially benefiting diabetic wound treatment. Additionally, considering Figure A, it is hypothesized that SCS enhances endothelial cell VEGF secretion, which in turn influences RAWs, via VEGFR1 to regulate chemokine expression and modulate the inflammatory state. Previous studies suggest that VEGFR1 plays a dual regulatory role by influencing both vascular permeability and the proangiogenic responses mediated by macrophages.

In summary, the regulation of angiogenesis within the immune microenvironment is a two-way process. The SAA hydrogel interacts with endothelial cells and macrophages to modulate the imbalanced inflammatory and angiogenic responses in a high-glycemic environment. The SAA hydrogel creates a microenvironment that facilitates tissue repair.

3.5. SAA hydrogel promoted diabetic rat oral mucosa defects healing

In vitro experiments demonstrated that SAA hydrogels are highly promising as wound dressings for treating diabetic oral mucosa defects. Consequently, a diabetic rat model with oral mucosa defects was established to assess the *in vivo* wound healing efficacy of SAA hydrogels. Fig. 8A illustrates the wound sites treated with PBS (blank control), AA, SAA, and iRegene® hydrogel. Wound progression in each group was documented and measured on days 1, 3, 7, and 9. Macroscopic examination revealed a reduction in wound size across all groups over time. Notably, the SAA hydrogel group demonstrated superior wound closure efficacy, achieving nearly complete healing within four days (Fig. 8a, b, c, f). The SAA group exhibited faster tissue growth compared to the iRegene® group on days 3 and 9, and compared to the control group on days 3, 6, and 9.

Additionally, the wound healing process was further analyzed via HE staining (Fig. 8d, e, g). HE staining images and epidermal thickness analysis indicated that by day three, the diabetic group had not formed a complete new epithelium. Furthermore, the epithelial thickness in the SAA group was significantly greater than in the AA and iRegene® groups. This trend continued on day seven, suggesting that SAA more effectively promotes upper re-epithelialization. By day seven, subcutaneous wound collagen deposition was observed in each group, attributed to the commercial product iRegene®. Concurrently, the enhanced re-epithelialization created a physical barrier within the wound microenvironment, effectively prevented excessive transdermal water loss and infection.

The efficacy of SAA hydrogel in repairing oral mucosal defects in rats was evaluated, using the commercially available intraoral wound dressing iRegene® as a positive control. The application of iRegene® to oral mucosal defects necessitated extra suturing due to poor adhesion, allowing foreign bodies to enter and increasing inflammatory cell presence. In contrast, SAA hydrogel could rapidly light-cure in-situ, conforming to various oral mucosal defect shapes and securing tightly to the tissue. This property prevented further irritation of the defects and induced M2 macrophage polarization to promote angiogenesis, accelerating oral mucosal wound healing.

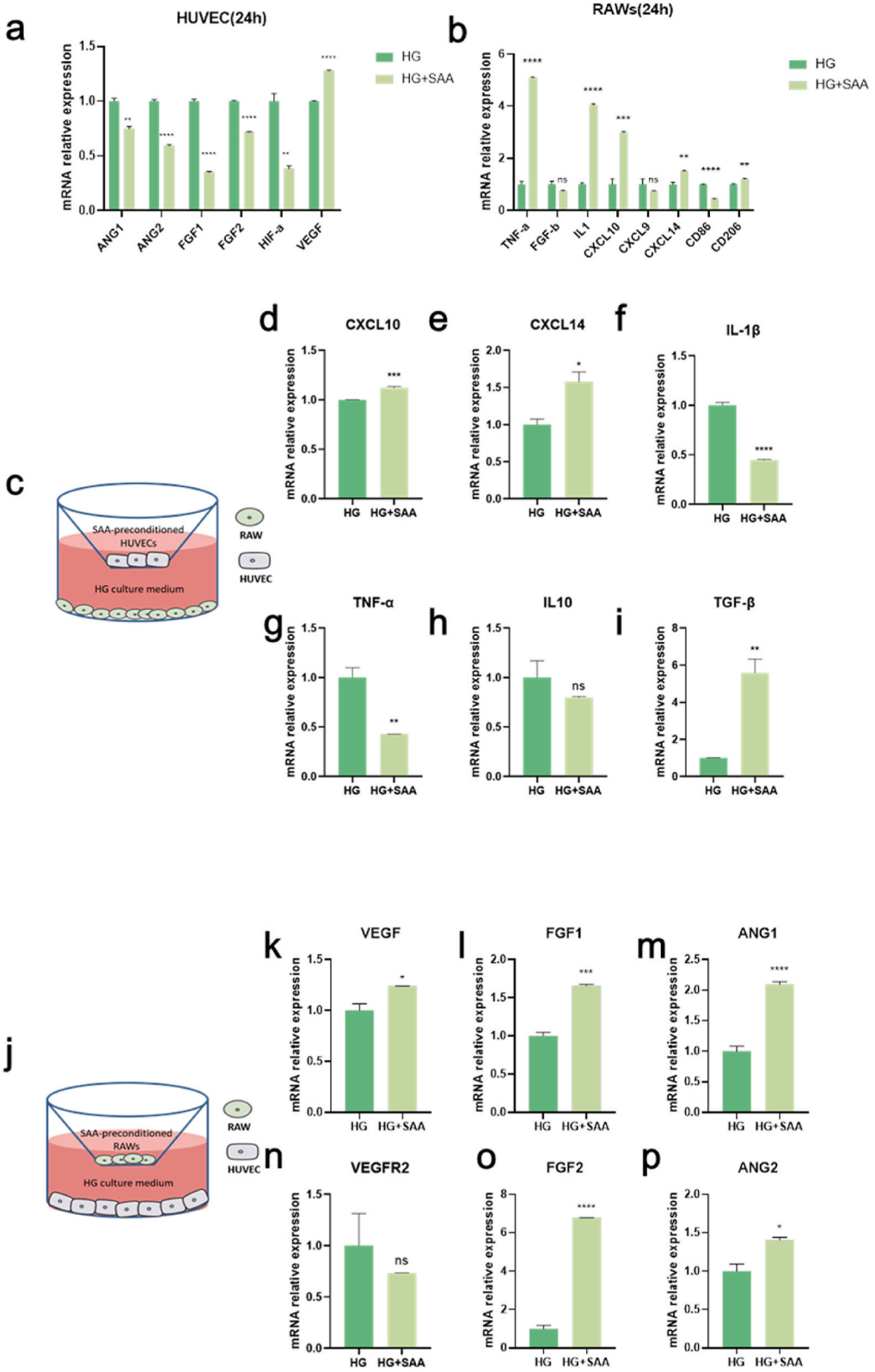

(caption on next page)

Fig. 6. Crosstalk between HUVECs and macrophages. (a) Angiogenic genes expression in HUVECs cocultured with SAA hydrogel for 24 h. (b) Relative gene expression of M1 phenotype in macrophages: CD86. Relative gene expressions of M2 phenotype in macrophages: CD206. RAW 264.7 cells were cocultured with SAA hydrogel for 12 and 24 h. (c) Schematic experimental design for investigating the effects of HUVECs cultured with SAA hydrogel on the polarization of RAW264.7 cells. Inflammation-related and angiogenic gene expressions of (d) CXCL2, (e) CXCL5, (f) IL-1β, (g) TNF-α, (h) IL-10 and (i) TGF-β, analyzed by qRT-PCR and (j) Schematic experimental design for investigating the effects of RAWs cultured with SAA hydrogel on the angiogenic function of HUVECs. Angiogenic -related genes expression of (k) VEGF, (l) FGF1, (m) ANG1, (n) VEGFR2, (o) FGF2, (p) ANG2 analyzed by qRT-PCR. (*P < 0.05, **P < 0.01, ***P < 0.005, ****P < 0.001).

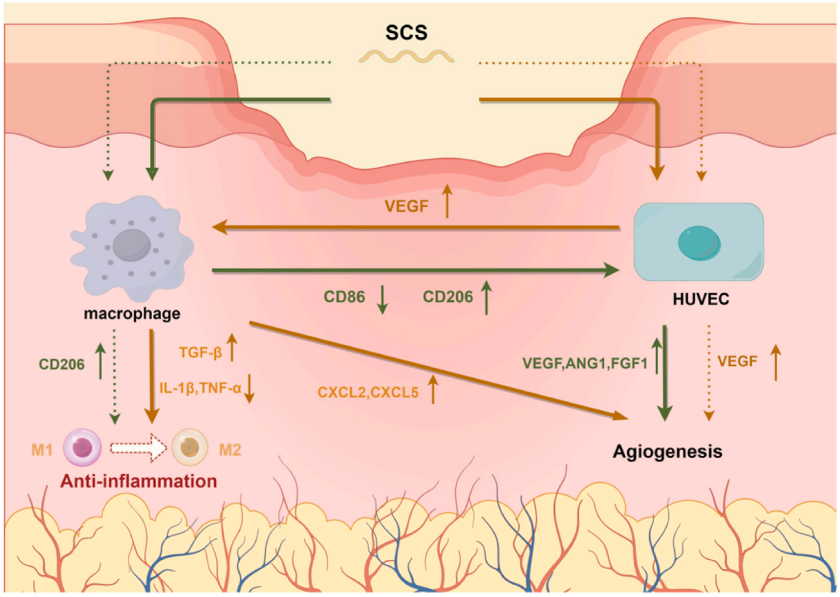

Fig. 7. Schematic of the SAA hydrogel regulating the crosstalk between macrophages and HUVECs to accelerate diabetic oral mucosa defects healing.

The mechanism by which SAA-induced mucosal healing occurs through angiogenesis is consistent with findings from cellular and rat models.

Experiments with a diabetic rat model confirmed that SAA gel promotes tissue repair and reduces wound healing time. These results suggest that SAA gel aids repair by blocking foreign bodies, encouraging local M2 macrophage polarization, and promoting angiogenesis at soft tissue defect sites. This creates a microenvironment favorable for vascular regeneration, minimal inflammatory infiltration, and tissue growth. In conclusion, these *in vivo* studies highlight the superior effectiveness of SAA hydrogel in treating diabetic oral mucosal defects.

3.6. Immunofluorescence and qRT-PCR analysis

Enhancing vascular regeneration in diabetic ischemic wounds is essential for better wound healing. Wound tissues were collected on days one and six post-treatment, and immunofluorescence staining (Fig. 9) and QPCR analysis (Fig. 10) were conducted. The results are presented in Fig. 10. First, immunofluorescence staining and analysis of VEGF were performed. VEGF expression significantly increased in the SAA hydrogel-treated group. By day 6, all groups exhibited an increase in VEGF expression, with SAA and iRegene® showing the most notable upregulation. This upregulation could be attributed to direct vascular regeneration by stem cells or angiogenesis via macrophage immune regulation, thereby enhancing tissue repair. These results confirm the efficacy of SAA hydrogel in boosting VEGF expression. Concurrently, CD31 and a-SMA served as vascular markers in the immunofluorescence analysis of the wound tissue. The experimental results showed that the expression trend of a-SMA and CD31 paralleled that of VEGF.

The qPCR results are depicted in Figures a–f. Initially (day 1), CD31 expression in the wounds of the SAA group surpassed that in the wounds of the AA group. CD31, a specific endothelial cell marker, suggests that an early dense vascular network aids later blood vessel formation. By a later stage (day 9), CD31 expression in the wounds of the SAA group remained higher compared to the AA group, aligning with the observed VEGF expression trend.

These *in vivo* findings highlight the substantial pro-angiogenic capacity of the SAA hydrogel-treated group compared to the control group.

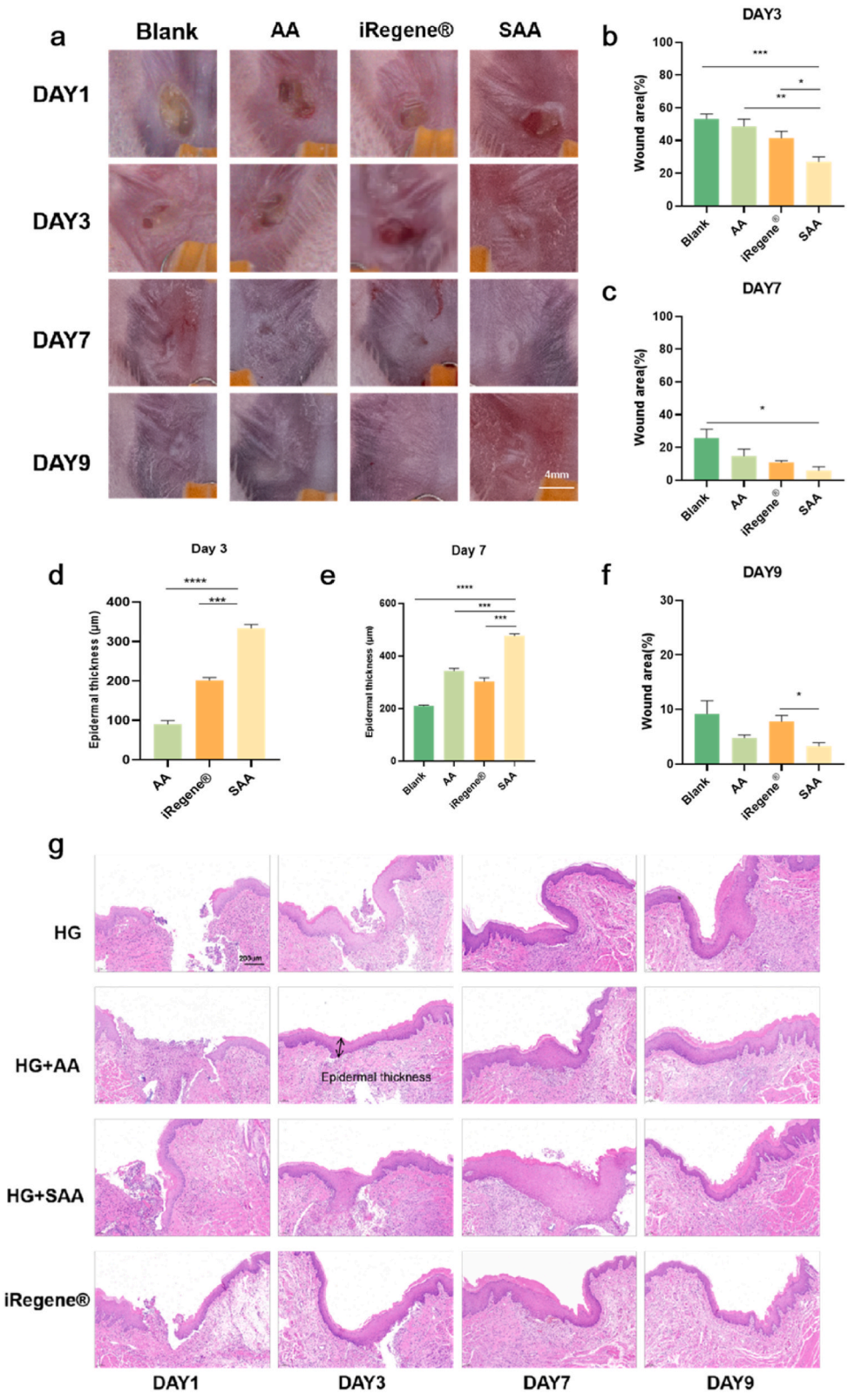

(caption on next page)

Fig. 8. SAA promotes the wound healing of oral mucosa in the diabetic rat model. (a) Representative optical images of diabetic rat oral mucosa defects across various treatment groups. Scale Bar: 4 mm, Wound-healing areas of rat oral mucosa were calculated on (b) Day3, (c) Day 6 and (f) Day 9 after treatment. (g) H&E staining showing the epithelial healing of the diabetic rat oral mucosa defects at (d) Day3 and (e) Day 7. Scale Bar: 100 μm (*P < 0.05, **P < 0.01, ***P < 0.005, ****P < 0.001).

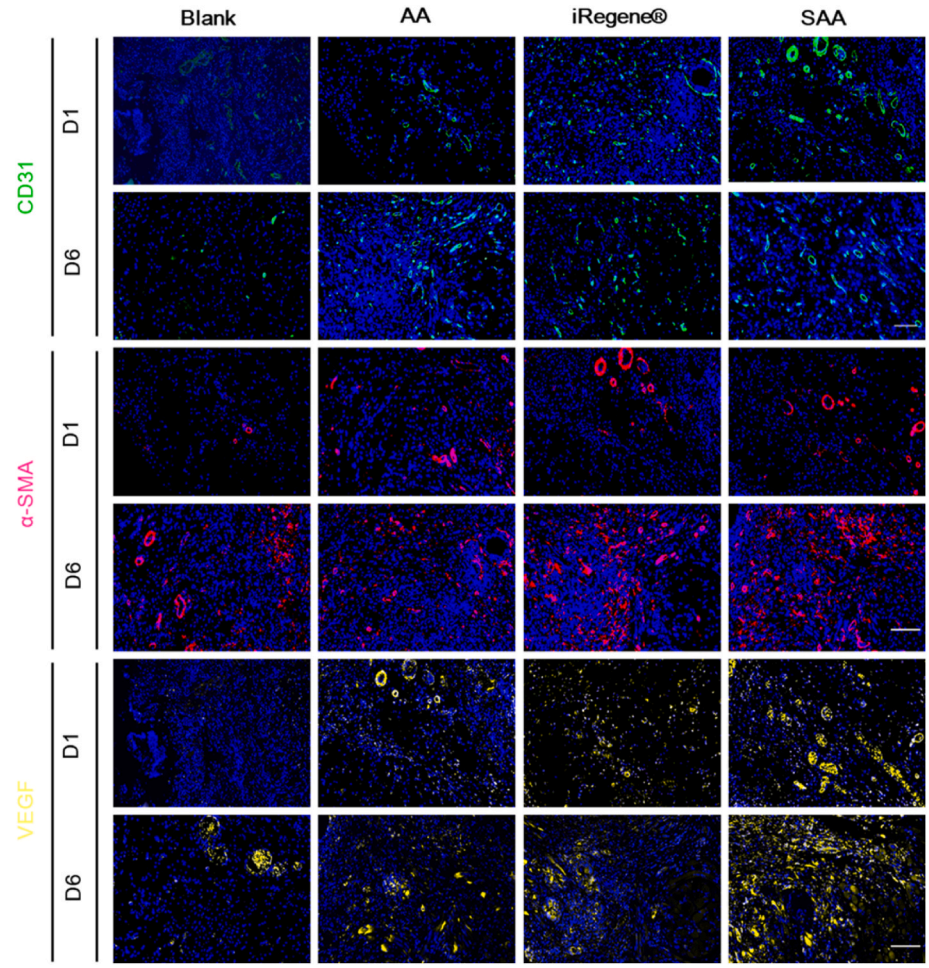

Fig. 9. IF staining of diabetic oral mucosa defects across various treatment groups. Scale Bar: 200 μm.

4. Conclusion

This study revealed that SCS-loaded hydrogel accelerates the healing of diabetic oral wounds through angiogenesis. This effect is further enhanced by the regulation of macrophage phenotype transition. Furthermore, the in situ photocross-linked AlgMA-AM hydrogel served as a dressing for oral wounds, offering suitable mechanical and adhesive qualities. AlgMA ensured sustained bioavailability, thereby enhancing therapeutic outcomes. In summary, the newly developed SAA hydrogel shows promise as a potential therapy for oral diabetic wounds. SAA hydrogel also has some limitations, such as the rapid release rate of SCS. SCS can be loaded into silica nanoparticles to achieve a sustained release effect and reduce its distribution in non-target areas [41]. Additionally, we did not take the risk of infection into account initially. Photothermal materials such as melanin nanoparticles could be a promising material. Upon exposure to near-infrared (NIR) light, these particles absorb light energy and convert it into localized heat to effectively kill bacteria [42].

Ethical statement

This work was approved by the Institute of Animal Care and Use Committee of Tongji University (no. [2023]-DW-48).

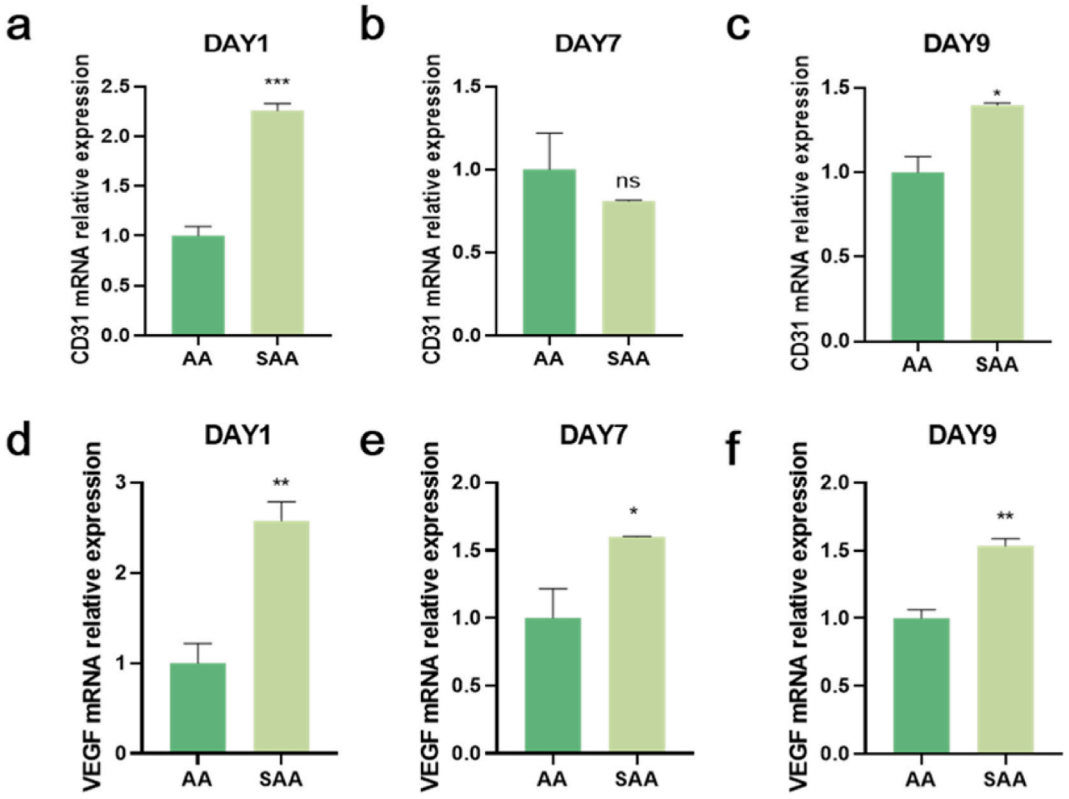

Fig. 10. Qpcr analysis of angiogenic genes expression in diabetic oral mucosa defects. (a–c) CD31, (d–f) VEGF. (*$P < 0.05$, **$P < 0.01$, ***$P < 0.005$, ****$P < 0.001$).

Data availability statement

Data will be made available on request.

Funding

This research was funded by the Science and Technology Committee Foundation of Shanghai (grant no. 23141902500) and the Natural Science Foundation of Shanghai (grant no. 19ZR462000).

CRediT authorship contribution statement

Shuwen Ding: Writing – original draft, Project administration, Methodology, Conceptualization. **Xiaohui Zhang:** Methodology, Conceptualization. **Gaopeng Wang:** Supervision, Resources. **Jiaying Shi:** Formal analysis. **Jiayu Zhu:** Resources. **Jiayu Yan:** Methodology. **Jing Wang:** Funding acquisition. **Junhua Wu:** Funding acquisition, Conceptualization.

Declaration of competing interest

The authors declare that they have no known competing financial interests or personal relationships that could have appeared to influence the work reported in this paper.

Acknowledgements

We acknowledge the invaluable discussions and constructive criticisms from anonymous reviewers, which significantly augmented the article's comprehensiveness and clarity.

References

[1] R.S. Apte, D.S. Chen, N. Ferrara, VEGF in signaling and disease: beyond discovery and development, Cell 176 (2019) 1248–1264, https://doi.org/10.1016/j.cell.2019.01.021.

[2] A. Alavi, R.G. Sibbald, D. Mayer, L. Goodman, M. Botros, D.G. Armstrong, K. Woo, T. Boeni, E.A. Ayello, R.S. Kirsner, Diabetic foot ulcers Part I. Pathophysiology and prevention, J. Am. Acad. Dermatol. 70 (1) (2014) e1, https://doi.org/10.1016/j.jaad.2013.06.055.

[3] F.M. Davis, L.C. Tsoi, R. Wasikowski, A. denDekker, A. Joshi, C. Wilke, H.P. Deng, S. Wolf, A. Obi, S. Huang, et al., Epigenetic regulation of the PGE2 pathway modulates macrophage phenotype in normal and pathologic wound repair, Jci Insight 5 (2020) e138443, https://doi.org/10.1172/jci.insight.138443.

[4] S. Patel, S. Srivastava, M.R. Singh, D. Singh, Mechanistic insight into diabetic wounds: pathogenesis, molecular targets and treatment strategies to pace wound healing, Biomed. Pharmacother. 112 (2019) 108615, https://doi.org/10.1016/j.biopha.2019.108615.

[5] M.J. Davis, S. Earley, Y.S. Li, S. Chien, Vascular mechanotransduction, Physiol. Rev. 103 (2023) 1247–1421, https://doi.org/10.1152/physrev.00053.2021.

[6] J. Benítez-Camacho, A. Ballesteros, L. Beltrán-Camacho, M. Rojas-Torres, A. Rosal-Vela, M. Jimenez-Palomares, I. Sanchez-Gomar, M.C. Durán-Ruiz, Endothelial progenitor cells as biomarkers of diabetes-related cardiovascular complications, Stem Cell Res. Ther. 14 (2023) 324, https://doi.org/10.1186/s13287-023-03537-8.

[7] A.M. Isidori, M.A. Venneri, D. Fiore, Angiopoietin-1 and Angiopoietin-2 in metabolic disorders: therapeutic strategies to restore the highs and lows of angiogenesis in diabetes, J. Endocrinol. Invest. 39 (2016) 1235–1246, https://doi.org/10.1007/s40618-016-0502-0.

[8] S. Obi, K. Yamamoto, J. Ando, Effects of shear stress on endothelial progenitor cells, J. Biomed. Nanotechnol. 10 (2014) 2586–2597, https://doi.org/10.1166/jbn.2014.2014.

[9] F. Alzoubi, B. Joseph, L. Andersson, Healing of soft tissue lacerations in diabetic-induced rats, Dent. Traumatol. 33 (2017) 438–443, https://doi.org/10.1111/edt.12372.

[10] C.P. Robinson, J. Cornelius, D.E. Bounous, H. Yamamoto, M.G. Humphreys-Beher, A.B. Peck, Characterization of the changing lymphocyte populations and cytokine expression in the exocrine tissues of autoimmune NOD mice, Autoimmunity 27 (1998) 29–44, https://doi.org/10.3109/08916939809008035.

[11] L. Tan, M.M. Zhong, Y.Q. Zhao, J. Zhao, M.A. Dusenge, Y. Feng, Q. Ye, J. Hu, Z.Y. Ou-Yang, N.X. Chen, et al., Type 1 diabetes, glycemic traits, and risk of dental caries: a Mendelian randomization study, Front. Genet. 14 (2023) 1230113, https://doi.org/10.3389/fgene.2023.1230113.

[12] D. Siegel-Axel, M. Barroso Oquendo, F. Gerst, F. Fend, R. Wagner, M. Heni, A. Königsrainer, H.U. Häring, A. Fritsche, E. Schleicher, et al., Extracellular matrix expression in human pancreatic fat cells of patients with normal glucose regulation, prediabetes and Type 2 diabetes, Int. J. Mol. Sci. 24 (2023), https://doi.org/10.3390/ijms241311169.

[13] K.I. Ko, A. Sculean, D.T. Graves, Diabetic wound healing in soft and hard oral tissues, Transl. Res. 236 (2021) 72–86, https://doi.org/10.1016/j.trsl.2021.05.001.

[14] A.I. Toma, J.M. Fuller, N.J. Willett, S.L. Goudy, Oral wound healing models and emerging regenerative therapies, Transl. Res. 236 (2021) 17–34, https://doi.org/10.1016/j.trsl.2021.06.003.

[15] R.J. Lamont, H. Koo, G. Hajishengallis, The oral microbiota: dynamic communities and host interactions, Nat. Rev. Microbiol. 16 (2018) 745–759, https://doi.org/10.1038/s41579-018-0089-x.

[16] T. Dong, N.M. Matos Pires, Z. Yang, Z. Jiang, Advances in electrochemical biosensors based on nanomaterials for protein biomarker detection in saliva, Adv. Sci. 10 (2023) e2205429, https://doi.org/10.1002/advs.202205429.

[17] P. Qin, J. Tang, D. Sun, Y. Yang, N. Liu, Y. Li, Z. Fu, Y. Wang, C. Li, X. Li, et al., Zn2+ cross-linked alginate carrying hollow silica nanoparticles loaded with RL-QN15 peptides provides promising treatment for chronic skin wounds, ACS Appl. Mater. Interfaces 14 (2022) 29491–29505, https://doi.org/10.1021/acsami.2c03583.

[18] E. Borie, E. Rosas, G. Kuramochi, S. Etcheberry, S. Olate, B. Weber, Oral applications of cyanoacrylate adhesives: a literature review, BioMed Res. Int. 2019 (2019) 8217602, https://doi.org/10.1155/2019/8217602.

[19] X. Tong, F. Yang, Recent progress in developing injectable matrices for enhancing cell delivery and tissue regeneration, Adv. Healthcare Mater. 7 (2018) e1701065, https://doi.org/10.1002/adhm.201701065.

[20] Y.L. Mao, Z.Y. Xu, Z.H. He, J. Wang, Z. Zhu, Wet-adhesive materials of oral and maxillofacial region: from design to application, Chin. Chem. Lett. 34 (2023) 107461, https://doi.org/10.1016/j.cclet.2022.04.059.

[21] T. Shen, K. Dai, Y. Yu, J. Wang, C. Liu, Sulfated chitosan rescues dysfunctional macrophages and accelerates wound healing in diabetic mice, Acta Biomater. 117 (2020) 192–203, https://doi.org/10.1016/j.actbio.2020.09.035.

[22] Y. Yu, K. Dai, Z. Gao, W. Tang, T. Shen, Y. Yuan, J. Wang, C. Liu, Sulfated polysaccharide directs therapeutic angiogenesis via endogenous VEGF secretion of macrophages, Sci. Adv. 7 (2021), https://doi.org/10.1126/sciadv.abd8217.

[23] H. Zhou, J. Qian, J. Wang, W. Yao, C. Liu, J. Chen, X. Cao, Enhanced bioactivity of bone morphogenetic protein-2 with low dose of 2-N, 6-O-sulfated chitosan in vitro and in vivo, Biomaterials 30 (2009) 1715–1724, https://doi.org/10.1016/j.biomaterials.2008.12.016.

[24] W. Zhang, B. Bao, F. Jiang, Y. Zhang, R. Zhou, Y. Lu, S. Lin, Q. Lin, X. Jiang, L. Zhu, Promoting oral mucosal wound healing with a hydrogel adhesive based on a phototriggered S-nitrosylation coupling reaction, Adv. Mater. 33 (2021) e2105667, https://doi.org/10.1002/adma.202105667.

[25] J. Zhang, S. Zhang, C. Liu, Z. Lu, M. Li, C. Hurren, D. Wang, Photopolymerized multifunctional sodium alginate-based hydrogel for antibacterial and coagulation dressings, Int. J. Biol. Macromol. 260 (2024) 129428, https://doi.org/10.1016/j.ijbiomac.2024.129428.

[26] S. Herber, J. Bomer, W. Olthuis, P. Bergveld, A. van den Berg, A miniaturized carbon dioxide gas sensor based on sensing of pH-sensitive hydrogel swelling with a pressure sensor, Biomed. Microdevices 7 (2005) 197–204, https://doi.org/10.1007/s10544-005-3026-5.

[27] V. Karageorgiou, D. Kaplan, Porosity of 3D biomaterial scaffolds and osteogenesis, Biomaterials 26 (2005) 5474–5491, https://doi.org/10.1016/j.biomaterials.2005.02.002.

[28] B. Huang, Y. Yuan, S. Ding, J. Li, J. Ren, B. Feng, T. Li, Y. Gu, C. Liu, Nanostructured hydroxyapatite surfaces-mediated adsorption alters recognition of BMP receptor IA and bioactivity of bone morphogenetic protein-2, Acta Biomater. 27 (2015) 275–285, https://doi.org/10.1016/j.actbio.2015.09.007.

[29] J. Sun, T. Chen, B. Zhao, W. Fan, Y. Shen, H. Wei, M. Zhang, W. Zheng, J. Peng, J. Wang, et al., Acceleration of oral wound healing under diabetes mellitus conditions using bioadhesive hydrogel, ACS Appl. Mater. Interfaces 15 (2023) 416–431, https://doi.org/10.1021/acsami.2c17424.

[30] Q. Wei, Y. Wang, K. Ma, Q. Li, B. Li, W. Hu, X. Fu, C. Zhang, Extracellular vesicles from human umbilical cord mesenchymal stem cells facilitate diabetic wound healing through MiR-17-5p-mediated enhancement of angiogenesis, Stem Cell Rev Rep 18 (2022) 1025–1040, https://doi.org/10.1007/s12015-021-10176-0.

[31] V. Falanga, Wound healing and its impairment in the diabetic foot, Lancet 366 (2005) 1736–1743, https://doi.org/10.1016/s0140-6736(05)67700-8.

[32] A.P. Veith, K. Henderson, A. Spencer, A.D. Sligar, A.B. Baker, Therapeutic strategies for enhancing angiogenesis in wound healing, Adv. Drug Deliv. Rev. 146 (2019) 97–125, https://doi.org/10.1016/j.addr.2018.09.010.

[33] K.L. Spiller, T.J. Koh, Macrophage-based therapeutic strategies in regenerative medicine, Adv. Drug Deliv. Rev. 122 (2017) 74–83, https://doi.org/10.1016/j.addr.2017.05.010.

[34] E. Zajac, B. Schweighofer, T.A. Kupriyanova, A. Juncker-Jensen, P. Minder, J.P. Quigley, E.I. Deryugina, Angiogenic capacity of M1- and M2-polarized macrophages is determined by the levels of TIMP-1 complexed with their secreted proMMP-9, Blood 122 (2013) 4054–4067, https://doi.org/10.1182/blood-2013-05-501494.

[35] M. Sharifiaghdam, E. Shaabani, R. Faridi-Majidi, S.C. De Smedt, K. Braeckmans, J.C. Fraire, Macrophages as a therapeutic target to promote diabetic wound healing, Mol. Ther. 30 (2022) 2891–2908, https://doi.org/10.1016/j.ymthe.2022.07.016.

[36] O.E. Rahma, F.S. Hodi, The intersection between tumor angiogenesis and immune suppression, Clin. Cancer Res. 25 (2019) 5449–5457, https://doi.org/10.1158/1078-0432.Ccr-18-1543.

[37] T. Chavakis, D.B. Cines, J.S. Rhee, O.D. Liang, U. Schubert, H.P. Hammes, A.A. Higazi, P.P. Nawroth, K.T. Preissner, K. Bdeir, Regulation of neovascularization by human neutrophil peptides (alpha-defensins): a link between inflammation and angiogenesis, Faseb. J. 18 (2004) 1306–1308, https://doi.org/10.1096/fj.03-1009fje.

[38] Y. Guan, L. Racioppi, S. Gerecht, Engineering biomaterials to tailor the microenvironment for macrophage-endothelium interactions, Nat. Rev. Mater. 8 (2023) 688–699, https://doi.org/10.1038/s41578-023-00591-9.

[39] J.L. Owen, M. Mohamadzadeh, Macrophages and chemokines as mediators of angiogenesis, Front. Physiol. 4 (2013) 159, https://doi.org/10.3389/fphys.2013.00159.

[40] H.G. Augustin, G.Y. Koh, G. Thurston, K. Alitalo, Control of vascular morphogenesis and homeostasis through the angiopoietin-Tie system, Nat. Rev. Mol. Cell Biol. 10 (2009) 165–177, https://doi.org/10.1038/nrm2639.

[41] P. Qin, J. Tang, D. Sun, Y. Yang, N. Liu, Y. Li, Z. Fu, Y. Wang, C. Li, X. Li, et al., Zn2+ cross-linked alginate carrying hollow silica nanoparticles loaded with RL-QN15 peptides provides promising treatment for chronic skin wounds, ACS Appl. Mater. Interfaces 14 (2022) 29491–29505, https://doi.org/10.1021/acsami.2c03583.

[42] Q. Jia, Z. Fu, Y. Li, Z. Kang, Y. Wu, Z. Ru, Y. Peng, Y. Huang, Y. Luo, W. Li, et al., Hydrogel loaded with peptide-containing nanocomplexes: symphonic cooperation of photothermal antimicrobial nanoparticles and prohealing peptides for the treatment of infected wounds, ACS Appl. Mater. Interfaces 16 (2024) 13422–13438, https://doi.org/10.1021/acsami.3c16061.